



Cite this: *Environ. Sci.: Nano*, 2025, 12, 5489

## Safe and sustainable by design-compliant LDPE food packaging embedding multicomponent nanomaterials for food protection

Andrea Brunelli, \*a Sara Trabucco,<sup>a</sup> Cástor Salgado,<sup>b</sup> Julian Jimenez Reinosa, José Francisco Fernandez, <sup>c</sup> Ana Serrano-Lotina,<sup>d</sup> Miguel A. Bañares, Magda Blosi, <sup>e</sup> Willie Peijnenburg, <sup>f,g</sup> Lya G. Soeteman-Hernandez, <sup>g</sup> Flemming R. Cassee, <sup>g,h</sup> Teresa Fernandes, <sup>i</sup> Angela Saccardo, <sup>j</sup> Shareen H. Doak, <sup>j</sup> Carlos Fito, <sup>k</sup> Ernesto Gonzalez Fernandez, <sup>k</sup> Jorge Salvador Hermosilla, <sup>k</sup> Irantzu Garmendia Aguirre, <sup>l</sup> Hubert Rauscher, <sup>l</sup> Vicki Stone, <sup>m</sup> Elisa Moschini, <sup>m</sup> Arianna Livieri, <sup>an</sup> Lisa Pizzol, <sup>n</sup> Danail Hristozov, <sup>o</sup> Antonio Marcomini<sup>a</sup> and Elena Badetti <sup>\*a</sup>

In response to the significant global crop losses caused by insect pests, which affect up to 40% of crops annually, there is an urgent need for safer food protection methods. This study addresses this need by proactively developing a safe and sustainable by design (SSbD) alternative to synthetic pesticides. Guided by the EC-JRC SSbD framework, the research focuses on an advanced low density polyethylene (LDPE) film embedding a multicomponent nanomaterial (MCNM), consisting of bentonite nanoclays and clove essential oil (BNT-CEO), designed to repel beetles. In detail, a three-step premarket safe-by-design assessment was performed. The first step was the safety assessment of the BNT-CEO material through i) physicochemical characterization, ii) screening for potential hazards of chemical precursors, and iii) preliminary *in vitro* toxicity tests. Afterwards, worker safety during both BNT-CEO synthesis and LDPE(BNT-CEO) production was assessed, analyzing dust generation and workers' potential exposure through an industrial hygiene survey followed by occupational monitoring. Lastly, consumers' safety was covered assessing the LDPE(BNT-CEO) film degradation and potential for migration of chemicals, by comparing pristine and accelerated-aged samples. Compliance with EU Regulation 10/2011 was verified by analyzing the migration of substances into food simulants. The integration of these safety evaluations early in the design process of BNT-CEO and LDPE(BNT-CEO) allowed confirmation of the material's compliance with regulatory limits and contributed to the validation of the assessment procedure as proposed by the SSbD framework. The approach here applied demonstrates how to successfully balance effective pest protection with minimal impact on consumers and workers, paving the way for the development of safer and sustainable food packaging solutions.

Received 30th April 2025,  
Accepted 9th November 2025

DOI: 10.1039/d5en00435g

rsc.li/es-nano

<sup>a</sup> Department of Environmental Sciences, Informatics and Statistics, Ca' Foscari University of Venice, Via Torino 155, 30170, Italy.

E-mail: andrea.brunelli@unive.it, elena.badetti@unive.it

<sup>b</sup> Encapsulae SL, Lituania 10, Castellón de la Plana, 12006, Spain

<sup>c</sup> Instituto de Cerámica y Vidrio (ICV), CSIC, Kelsen 5, 28049 Madrid, Spain

<sup>d</sup> Instituto de Catálisis y Petroleoquímica (ICP), CSIC, Marie Curie 2, 28049 Madrid, Spain

<sup>e</sup> National Research Council, Institute of Science, Technology and Sustainability for Ceramic Materials ISSMC-CNR, Faenza, Italy

<sup>f</sup> Institute of Environmental Science, Leiden University, Leiden, The Netherlands

<sup>g</sup> National Institute for Public Health and the Environment (RIVM), Bilthoven, The

Netherlands

<sup>h</sup> Institute for Risk Assessment Sciences – Division Toxicology, Utrecht University, Utrecht, The Netherlands

<sup>i</sup> Heriot Watt University, UK

<sup>j</sup> Institute of Life Science, Swansea University Medical School, Swansea, UK

<sup>k</sup> Technological Institute of Packaging, Transport and Logistics, Paterna, Spain

<sup>l</sup> European Commission, Joint Research Centre, Ispra, Italy

<sup>m</sup> Institute of Biological Chemistry, Biophysics and Bioengineering, Heriot-Watt University, Edinburgh, UK

<sup>n</sup> GreenDecision srl, Cannaregio 5904, 30121 Venezia (VE), Italy

<sup>o</sup> EMERGE Ltd, Sofia, Bulgaria



## Environmental significance

Advanced materials (AdMas) offer innovative solutions for food technology systems, providing enhanced functional properties, improving food quality and safety, with a focus on environmental, economic and social sustainability. These sustainable alternatives help reduce reliance on conventional plastics and synthetic pesticides, which are major contributors to microplastic pollution and ecosystem degradation. Demonstrating this potential, an innovative LDPE food packaging material – incorporating clove essential oil-loaded bentonite nanoclays – has been designed to effectively prevent food loss by repelling beetles. Guided by the EC-JRC Safe and Sustainable by Design (SSbD) framework, a safe-by-design assessment of this AdMa was carried out, leading to optimal protection from pests while minimizing risks for both workers and consumers. The results of this case study could form the basis for a roadmap showing how to exploit the SSbD approach to generate a multitude of next gen, nanotechnology-containing materials suitable for the most diverse industrial functions and applications.

## 1. Introduction

The production and consumption of food, which can undergo spoilage processes due to microbial, chemical, or physical processes, are central to any society, with social, economic and, in many cases, environmental consequences.<sup>1–3</sup> Food preservation is thus essential to maintaining its quality over time. The European Food Safety Authority (EFSA) and the European Centre for Disease Prevention and Control (ECDC) disclosed more than 5700 foodborne outbreaks in the EU in 2022, a 44% increase compared with 2021 (EFSA and ECDC, 2023).<sup>4</sup> Concerning food safety, EU legislation requires that any material or article intended to come into contact with food (namely food contact material, FCM), including food packaging and containers, machinery to process food or kitchenware and tableware, must not release chemicals into food in quantities that could be harmful to human health.<sup>5</sup> To face this challenge, manufacturers, retailers, consumers, and regulatory bodies are demanding higher quality standards and new strategies to protect, monitor and trace food quality throughout the supply chain,<sup>1,6</sup> as also recently advocated also through the European Green Deal.<sup>7</sup> Assessing the impact of food packaging on human health and the environment requires understanding the chemical composition of the packaging material as well as determining which substances can migrate into food and at which concentration levels.<sup>8</sup> In this regard, food packaging plays a vital role in ensuring food safety throughout its life cycle and maintaining the benefits of food processing, allowing food to travel safely over long distances or to be stored in warehouses or in retail stores for long periods.<sup>9,10</sup> However, even if packed, cereal-based dry foods, such as rice, flour or legumes, may be infested by insects,<sup>11</sup> among which the most destructive ones are Coleoptera (beetles) and Lepidoptera (moths).<sup>12</sup> The ability of insects to penetrate through food packaging and to degrade/eat food has been documented since the 1940s.<sup>13,14</sup> The Food and Agriculture Organization of the United Nations (FAO) recently estimated that insect pests can infest each year as much as 40% of the world's crop yield, resulting in a decrease in food quality and in an increase in foodborne diseases that can impact human health and well-being.<sup>15</sup> Recent advances in food packaging have led to the development of active, intelligent, and smart packaging materials that improve food quality, ensure air-tightness,

extend shelf life and provide real-time information about the conditions of the food products.<sup>16</sup> Food packaging materials vary to meet the technical demands of the supply chain and marketing needs (such as brand identity and consumer information). Across the different types, plastics are among the most popular food packaging materials, given their lightweight, flexibility, versatility, and good barrier properties. To even improve these properties, a wide range of compounds are added to the different food packaging materials, ranging from natural substances to intentionally produced chemical additives. There is a wide set of substances used in food packaging for their antioxidant, antimicrobial and anti-inflammatory properties, ranging from synthetic compounds (e.g., *N,N*-diethyl-*meta*-toluamide, chlorine dioxide, ethanol, sulfur dioxide, *etc.*), characterized by some concerns on performance durability and (eco) toxicological effects, to natural substances (e.g., methyl salicylate, cinnamon, and propionic acid).<sup>17–19</sup>

A very promising category of natural extracts is essential oils (EOs), such as clove, neem, citronella, oregano and thyme oils. Numerous studies demonstrate the adverse effects of EOs against pathogens, which can cause post-harvest diseases in fruits and vegetables.<sup>20</sup> A literature analysis of applications of EOs in agriculture and agricultural products through network maps created using VOSviewer software revealed that they are mostly used for their antibacterial and insecticidal properties, while no evidence emerged for nematocidal and acaricidal activity.<sup>21</sup> However, their efficacy is strictly linked to the evaporation degree of their volatile molecules, due to their high vapor pressure (the higher the vapour pressure, the faster the evaporation and thus the loss of performance). Therefore, their high volatility and hence rapid degradability have made their use limited, calling for further efforts in a better controlled release of organic molecules. To address this issue, advanced materials (AdMas), including engineered multi-component nanomaterials (MCNMs), designed to present novel or enhanced properties and better performance in products and processes compared to conventional materials, are attracting great attention in this field.<sup>22</sup> Examples of nanomaterials (NMs) for food protection and safety include Ag, ZnO, TiO<sub>2</sub>, nanoclays, nano-starch and carbon nanotubes (CNTs).<sup>17,23–26</sup> Ag and ZnO NMs are generally used as antimicrobial or anti-pest agents; nanoclays or layered silicates for enhanced barrier properties to gases, moisture, and volatile



compounds;  $\text{TiO}_2$  NMs are often employed as photocatalysts for the degradation of hazardous substances or microorganisms.<sup>27</sup> Nevertheless, despite scientific efforts in developing innovative NM-based food packaging, concerns on the potential adverse effects of NMs towards human health and the environment still exist, and there is no univocal opinion on the NM toxicological profile yet.<sup>28</sup> Indeed, several factors can influence the biokinetic behaviour and/or the toxicological responses of NMs, such as chemical composition, particle size, shape, surface area, concentration, and exposure time, as well as the surrounding medium or environmental conditions. At the regulatory level, the EFSA recently published the Guidance on risk assessment of the application of nanoscience and nanotechnologies in the food and feed chain, human and animal health.<sup>29</sup> This guidance clarifies when nanospecific risk assessment is needed for particulate materials used in the food and feed chain, and what such a risk assessment entails. It addresses nanospecific aspects of physicochemical characterization, hazard identification and exposure assessment.

A promising solution which extends the duration of EO release over time is the adsorption onto inorganic porous materials. Examples of such materials are EO-clay hybrids, which leverage the high surface area and layered structure of clays, coupled with the antimicrobial and antioxidant properties of EOs.<sup>30</sup> The typical structure of clays makes them ideal as sorbents and nanocarriers for EOs, enabling controlled EO release while protecting it from early degradation.<sup>31-34</sup> Currently, EO-based materials' global market uptake is still limited since a favorable cost-benefit balance has not yet been achieved. However, their unique features make them appealing as a viable solution for food packaging, opening the possibility of a wider global distribution in the near feature, especially if developed in agreement with new requirements in terms of safety and sustainability. Recently, the Joint Research Center (JRC), the European Commission's science and knowledge service, published the EU's Safe and Sustainable by Design (SSbD) framework,<sup>35</sup> with the objective of driving the innovation of chemicals and materials through the voluntary application of safety and sustainable principles at early R&D innovation stages. A preliminary qualitative safety and sustainability assessment of an advanced food packaging material for food protection was published by Pizzol *et al.*, 2023.<sup>36</sup> The authors compared two innovative EO clay-based materials as anti pests, developed for application onto light density polyethylene (LDPE) for food packaging. Both materials consisted of nanodrops of food-grade essential oil (EO), anchored to nanoclays (either E-558 bentonite layered nanoclays or E-562 sepiolite fibrillary nanoclays). The EO-clay-based materials were then encapsulated by an organic acid (E-297 fumaric acid) and subsequently incorporated into an LDPE matrix during the thermoforming of the food packaging.<sup>37</sup> The life cycle analysis results showed that the innovative EO-clay materials offer significant advantages over their conventional counterparts, making strategically

beneficial investigating further developments. In this context, the current work aims to integrate the safety and sustainability aspects related to the innovative food packaging as addressed by Pizzol *et al.*, 2023,<sup>36</sup> with a detailed investigation of the safety aspects of the specific case study. This will help to assist SMEs in their decision-making in agreement with the SSbD initiative.

Recognizing the crucial importance of food safety, a pre-market screening was conducted to evaluate workers and consumers' exposure to the innovative material. The LDPE(BNT-CEO) material constitutes an exemplary case study for the implementation of the EU-JRC SSbD framework, as it encompasses several critical challenges – namely, the complexity arising from multiple components, their interactions with both the polymeric matrix and the food, and the potential migration of chemicals into the food – which, when systematically addressed, can inform the design of safer and more sustainable materials.

## 2. Materials and methods

### 2.1 Advanced material preparation and performances

**2.1.1 AdMa synthesis.** The design of the investigated AdMa consisted of an LDPE film embedding bentonite nanoclays (namely BNT hereinafter) loaded with drops of clove essential oil (CEO). LDPE is generally used in a wide range of applications, especially in food packaging because of its flexibility and toughness, high resistance to moisture, cost-effectiveness and transparency.<sup>38</sup> BNT with a layered platelet morphology, 1.6 nm in thickness and 600 nm in length, was purchased from SEPIOLSA (Minersa Group). CEO (84% eugenol and 16%  $\beta$ -caryophyllene) was a plant-derived extract purchased from Arocival (Aromes Citrics Valencians S.L., Spain). All the other reagents and chemicals used were of analytical reagent grade (Merck, KGaA, Darmstadt, Germany).

The BNT-CEO MCNM synthesis started from BNT, which was separately purified and loaded with CEO to be further embedded in a commercial grade light density polyethylene (LDPE) film (SABIC® LDPE 2101N0W from SABIC). A summary of the different steps from the BNT-CEO synthesis to the LDPE(BNT-CEO) extrusion is briefly described herein and schematically displayed in Fig. 1. In detail, 411 g of raw BNT and 8.4 g of anhydrous sodium carbonate ( $\text{Na}_2\text{CO}_3$ ) were individually dispersed in separate containers, each containing 2.9 L of distilled water. Both suspensions were independently mixed with a hand blender for 10 min and left to stand for 24 h. Afterwards, the suspensions were stirred with a Cowles type mixer at 1200 rpm for 20 min and filtered with a 100  $\mu\text{m}$  sieve. Both slurries were magnetically filtered, and then transferred together to a single 15 L pot equipped with a mechanical mixer and an Ultra-Turrax homogenizer. Then, 25 g of citric acid was mixed with 250 g of clove essential oil diluted in 100 g of ethanol and then added to the mixture. The slurry was mixed for 2 h and vacuum filtered with a Büchner funnel and then dried at 80 °C for 48 h. The modified clay was then ground, sieved (100  $\mu\text{m}$ ) and



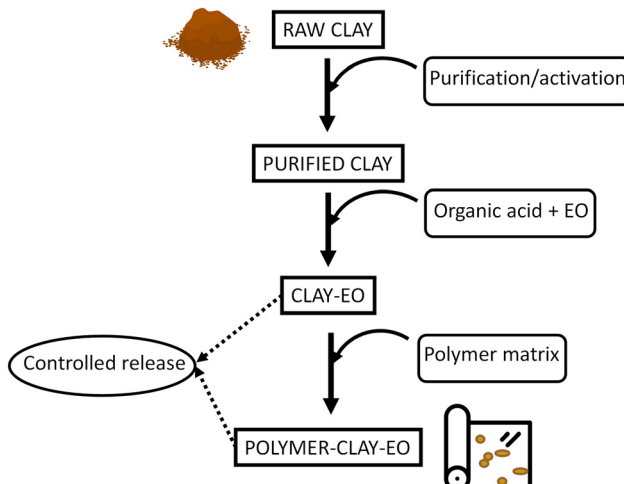


**Fig. 1** Scheme of the production process of the AdMa (LDPE(BNT-CEO) film).

thermally treated at 120 °C for 3 h to obtain the modified BNT powder with 10 wt% of CEO.

To incorporate BNT-CEO into LDPE, polymer pellets were mixed with the BNT-CEO in a 90:10 LDPE:BNT-CEO ratio using an acoustic mixer (Resodyn LabRAMII H) and a masterbatch was prepared by extrusion at 170 °C. Films with a thickness of 90 µm were blown to obtain LDPE(BNT-CEO) composites with 1, 2 and 5 wt% of BNT-CEO. The thickness of the films was measured with a Mitutoyo Absolute meter, with a resolution of 0.001 mm, by performing 5 measurements in different regions of the film. The obtained films were wound onto reels and stored in sealed containers protected from light. No material treatment was required before conducting the corresponding tests.

**2.1.2 Insect barrier performance test.** A preliminary barrier performance test was conducted as a first indication on the film functionality as an insect repellent. The material's other functional properties (such as moisture and oxygen barrier), mechanical strength and durability (such as tensile strength), despite being acknowledged to be relevant for food packaging, were not the focus of this study. Future research will explore these properties to ensure that the material meets all necessary standards for commercial use.

The barrier performance of LDPE films containing BNT-CEO was evaluated in a preliminary screening assay using the red flour beetle *Tribolium castaneum* as a model pest for real-world food production. This species was selected for two key characteristics: i) exceptional desiccation resistance due to its specialized cryptonephridial complex, which allows it to survive in extremely dry environments typical of stored products; ii) well-documented multifaceted insecticide resistance, both making it a robust test organism.<sup>39</sup>

Within the screening assay, LDPE films embedded with three different concentrations of BNT-CEO (1%, 2%, and 5% w/w) have been tested and compared to standard LDPE as a control. In addition, the assay was designed to explore how different film configurations could better prevent insect

infestation. Both non-microperforated and microperforated films were tested, each with a 60 µm thickness. For each trial, a flour-filled sachet was sealed with a test film and placed inside a glass container with 20 adult *T. castaneum* beetles to assess the film's ability to limit insect entry. The number of beetles inside and outside the films was recorded daily for seven days under a 12 hour light/dark photoperiod. For each BNT-CEO concentration and film type, 10 replicates were conducted, along with 10 control replicates. All insects belonged from a single laboratory colony maintained under optimal growth conditions. Experiments were carried out at room temperature and 55–60% relative humidity. At the end of the exposure period, cumulative values were used to assess insect penetration. Results were analyzed using one-way ANOVA followed by Tukey's honestly significant difference (HSD) test for multiple comparisons. Statistical significance was evaluated at  $\alpha = 0.05$ .

## 2.2 Safety assessment approach

The methodological approach adopted aligned with the 3 steps of the EU-JRC SSbD framework and covered the safety aspects of 1) synthesis, 2) production and 3) use phases of the newly marketed AdMa (Fig. 2). The physicochemical characterization covered all three steps of this study.

The safety assessment began by gathering fundamental information for step 1 of the EU-JRC SSbD framework, which focuses on hazard assessment. This was accomplished by: i) physicochemical characterization of the AdMa, including all the components/ingredients of the final product; ii) hazard assessment of the BNT-CEO precursors (*i.e.*, bentonite clay, clove essential oil, citric acid and sodium carbonate) using classification, labelling and packaging (CLP) data; iii) *in vitro* assays on both the precursors and BNT-CEO to fill the toxicological data gaps.

The human health and safety aspects in the chemical/material production and process phases (step 2 of the EU-JRC SSbD framework) consisted of: i) preliminary dustiness testing during the handling and processing of the AdMa; ii) an occupational exposure assessment through a three-tiered approach *via* an air monitoring campaign.

Lastly, the safety of the AdMa was addressed in step 3 of the EU-JRC SSbD framework (human health and environmental aspects in the final application phase), investigating the potential migration of hazardous substances from both pristine and accelerated aged LPDE(BNT-CEO) films.

## 2.3 Hazard assessment

### 2.3.1 Advanced material physicochemical characterization.

Physicochemical characterization of the different constituents of the AdMa was performed following the different steps of the production process. First, the specific surface area and total pore volume of BNT were measured *via* the Brunauer, Emmett and Teller method (BET) by using a Micromeritics model ASAP 2460 with nitrogen as carrier gas.



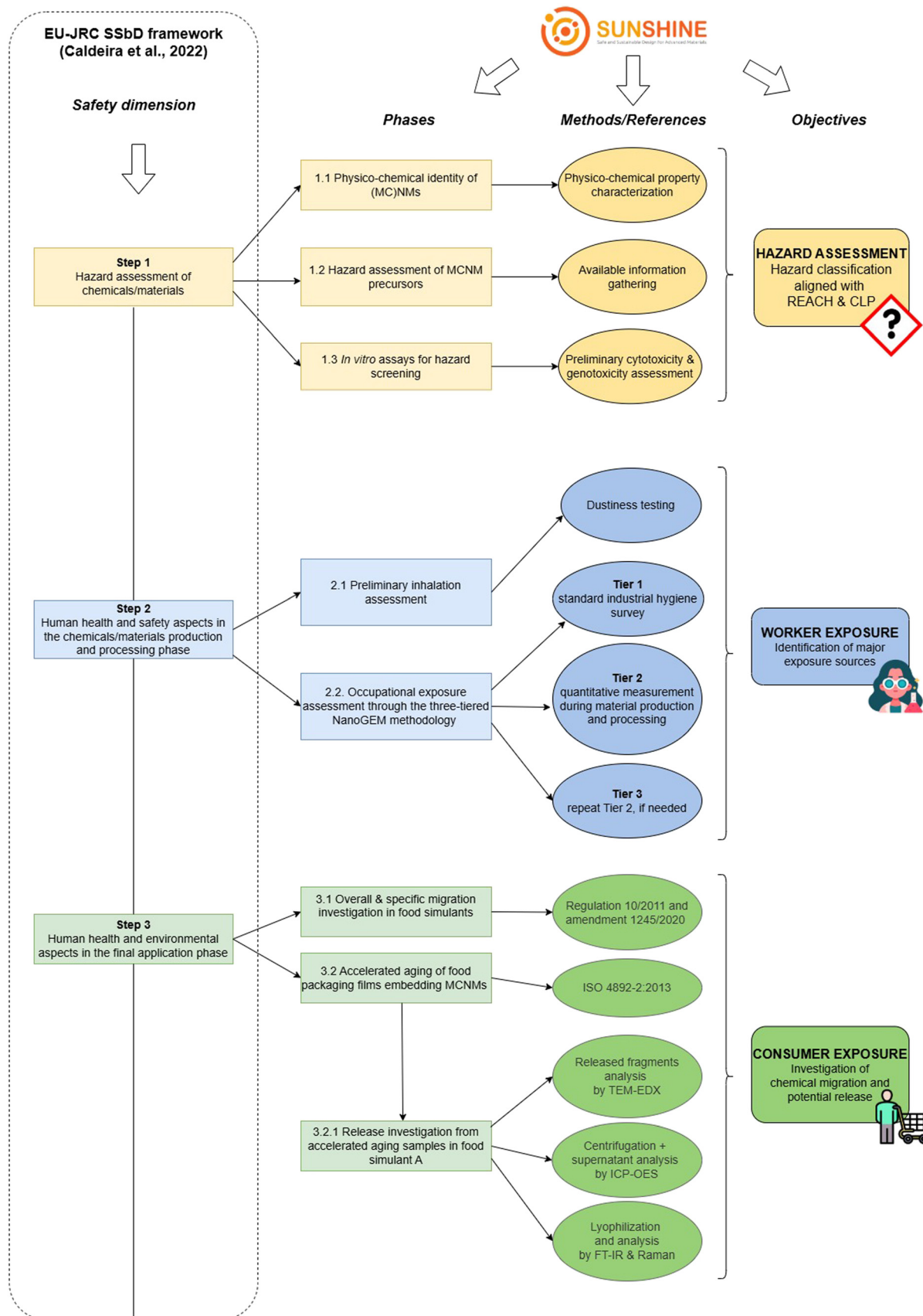


**Fig. 2** Graphical representation of the SUNSHINE methodology applied to address the safety aspects (as identified by the EU-JRC SSB framework) of the BNT-CEO-based LDPE case study. Ellipses display the methods adopted within each phase of the assessment, in agreement with standard or recommended procedures.



Samples were previously degassed at 150 °C under dynamic vacuum for 2 hours. Cation exchange capacity (CEC) was determined through the methylene blue method. 0.5 g of clay was weighed and suspended in a 2 wt% Na<sub>4</sub>P<sub>2</sub>O<sub>7</sub> solution. Then, 0.5 N H<sub>2</sub>SO<sub>4</sub> solution was added, and the mixture was stirred for 5 min. The suspension was titrated with methylene blue (Sigma Aldrich) until the first drop of excess was detected. The amount of carbonate present in BNT was determined through a Bernard calcimeter, measuring the volume of CO<sub>2</sub> released after adding a HNO<sub>3</sub> (60%) solution to the clay.

Powder X-ray diffraction (XRD) patterns were recorded on a Bruker D8 Advance diffractometer with a fast LynxEye detector and Cu K $\alpha$  radiation ( $\lambda = 1.5406 \text{ \AA}$ ). Data were collected over a  $2\theta$  range of 5° to 70° with a step size of 0.05°. The samples were analyzed as finely ground powders in low-background holders. The EVA software (Bruker AXS) and the JPCD2.2CA database were used to identify the mineralogical composition. Semi-quantitative phase composition and amorphous content were estimated based on the full width at half maximum (FWHM) of characteristic reflections.

Then, the morphology and the loading efficiency of CEO drops within BNT were investigated by using field emission scanning electron microscopy (FE-SEM) Hitachi S-4700 equipment and an optical microscope (Z-Axiopot). The molecular interactions between BNT and CEO were studied using a Thermo Nicolet Nexus 670 Fourier-transform infrared (FTIR) spectrophotometer equipped with a Smart Orbit Single Reflection Diamond ATR (attenuated total reflection) accessory, from 4000 to 400 cm<sup>-1</sup> for 64 scans with 4 cm<sup>-1</sup> resolution. In addition, thermogravimetric analysis (TGA) was performed to investigate the presence of CEO within the nanoclays by weight loss through a TGA Q50 (from TA Instruments) apparatus. The temperature program used was set up experimentally from 30 °C to 900 °C at 10 °C min<sup>-1</sup>. The samples (masses ranging between 8 and 30 mg) were placed in a platinum crucible and the measurements were done in dynamic mode in air for the BNT-CEO and nitrogen for the LDPE(BNT-CEO) films (flow rate of 60 mL min<sup>-1</sup>). All data generated were elaborated with Origin 8.5 software.

In addition to the basic physicochemical characterization of BNT, CEO loss from BNT-CEO was indirectly estimated through UV-vis spectroscopy (Lambda950, Perkin Elmer), by measuring the release of eugenol over time. For this purpose, 2 g of BNT-CEO was placed on Petri dishes and exposed to air both at room temperature (RT) and at 80 °C. Then, 20 mg of each sample was collected at different times for a total of 30 days. The samples were extracted in triplicate with methanol (HPLC grade) in sealed flasks, alternating 5 min of magnetic stirring, 5 min of ultrasonication bath and another 5 min of magnetic stirring. The supernatant was filtered (PTFE filters with 0.45  $\mu\text{m}$  pore size) and the amount of eugenol released was measured with a UV-vis spectrometer (between 250 nm and 400 nm with a resolution of 1 nm).

Physicochemical characterization of both pristine LDPE and LDPE(BNT-CEO) films was also performed by FTIR and Raman spectroscopy (DXRTM3, Thermo Scientific™) to investigate the surface morphology. Furthermore, eugenol release from the LDPE(BNT-CEO) films after 5 and 12 months was studied by measuring the reduction of the absorption band at 280 nm *via* UV-vis spectroscopy, on 10  $\times$  5 cm films exposed to air under laboratory conditions.

**2.3.2 Literature toxicological information on the material precursors.** Since the LDPE(BNT-CEO) film under design is an innovative material, the toxicological information available from the literature is only related to its precursors. Therefore, a preliminary hazard assessment of the ingredients used for the BNT-CEO synthesis was performed, based on the CLP Regulation 1227/2008 and on the Registration, Evaluation, Authorization and Restriction of Chemicals (REACH) Regulation 1907/2006. The precursors investigated were: BNT powder (CAS no. 1302-78-9), clove essential oil (CAS no. 8000-34-8), citric acid (CAS no. 77-92-9) and sodium carbonate anhydrous (CAS no. 497-19-8).

**2.3.3 *In vitro* toxicity testing of BNT-CEO.** In addition to the preliminary hazard assessment, cytotoxicity and genotoxicity screenings of BNT, citric acid (CA) – as a representative organic acid used in the synthesis – CEO and BNT-CEO were performed on TK6 cells. TK6 is a human lymphoblast cell line routinely used for the *in vitro* genotoxicity testing of chemicals and NMs *via* the cytokinesis-block micronucleus (CBMN) assay (OECD Test Guideline (TG) 487). The OECD TG487 has been adapted for use with NMs<sup>40</sup> and was followed for this experimental work. Cytotoxicity was evaluated *via* relative population doubling (RPD), which monitors the cell growth and compares it with the untreated control before and after exposure to BNT-CEO (24 h). At the same time, the CBNM assay provides a measure of induced DNA damage following exposure, recorded as the percentage of micronuclei detected in binucleated cells. Methyl methane sulfonate (a known genotoxin) was included as a positive control. *In vitro* testing on TK6 cells requires that BNT-CEO remains stably dispersed for at least 24 hours. However, when dispersed on its own, BNT-CEO begins to precipitate within 10 minutes. To address this issue, the stability of the BNT-CEO suspension was enhanced by combining BNT-CEO with xanthan gum (XG) in a 5:1 ratio and then dispersing the mixture in 0.05% bovine serum albumin (BSA). XG is intended to increase the viscosity of the medium without altering the effects exerted by the BNT-CEO. The different concentrations of BNT-CEO tested were determined according to the mass weight of the BNT-CEO without XG, as the stabilizer was only used to improve the experimental conditions within the *in vitro* hazard assessment and is not a component of the final material used for commercial applications.

BNT-CEO-XG was tested alongside its individual components and XG to rule out any potential for additive or synergistic effects when they are combined.



## 2.4 Occupational exposure assessment

Occupational safety and health (OSH) aspects were first evaluated through dustiness testing to provide an indication on the potential generation of airborne dust particles during handling and processing of BNT-CEO in the powder form. Afterwards, a three-tiered methodology for occupational exposure assessment recommended by different authors and institutions<sup>41–45</sup> was employed to address both the production and processing of the BNT-CEO powder and the LDPE(BNT-CEO) film (Fig. 3). This three-tiered methodology was already applied within the SUNSHINE project to a BNT-CEO-based material used in construction.<sup>46</sup>

The dustiness test was performed by pre-conditioning the powder at room temperature (20–22 °C) in a humidified box (50–55% relative humidity) for 2 days. The dustiness tester was filled with 0.4 g of powder, putting the material into the funnel as far as possible. The top of the tester was replaced and connected to the analyzers and clean air inlet. The flow was increased from 0 to 600 mL min<sup>-1</sup> in ±10 s. Aerosol formation was then measured by means of a scanning mobility particle sizer (SMPS) and an aerodynamic particle sizer (APS), covering the respirable particle range (0–10 µm): 1) the SMPS measured particles in the range between 14 and 670 nm, expressing it as the count median diameter (CMD) and particle number; 2) the APS measured particles in the range between 0.52 and 20 µm, expressing it as the mass median aerodynamic diameter (MMAD) and particle number. The temperature and the relative humidity of air were also measured for 10 s. In a 90 min test with 3 min measurements, the movement of the substance was observed to gauge the energy needed for particle release. The observed states ranged from stationary (high energy required due to stickiness, large particles, or high friction) to full fluidization (low energy required due to small particles and/or low friction).

With regard to the three-tiered methodology, tier 1 comprised a standard industrial hygiene survey through the administration of questionnaires prepared by following the EN 17058:201830 “Workplace exposure – Assessment of

exposure by inhalation of nano-objects and their aggregates and agglomerates”.<sup>47</sup> The questionnaires were filled in by Instituto de Cerámica y Vidrio, Spanish National Research Council (ICV-CSIC) and Encapsulae S.L., who developed both the BNT-CEO synthesis and the LDPE(BNT-CEO) food packaging. Target areas, processes, sources or activities, from which any release could occur, were identified. Based on the results from the survey, an occupational exposure assessment was performed as the tier 2 step, focusing on both the BNT-CEO synthesis and the LDPE(BNT-CEO) film production and processing. According to the definition of exposure scenarios (ES) by the European Chemicals Agency (ECHA),<sup>48,49</sup> two different exposure scenarios were identified: ES1 = BNT-CEO synthesis, which includes kneading of the different nanomaterials/chemicals used, milling, sieving, weighing and mixing of the BNT-CEO with polyethylene particles and bagging; ES2 = LDPE(BNT-CEO) film production and processing, which comprises the melting of the micronized mixture in an extruder, pellet drying and plastic film blowing. The location and the rooms in which the different activities were performed are displayed in Fig. S1–S4.

The potential exposure to particles during both the BNT-CEO synthesis and the LDPE(BNT-CEO) film production and processing was evaluated over time. The particle number and mass concentration both in air and in the personal breathing zone (*i.e.*, PBZ, around 30 cm from the respiratory tract) of the workers were determined by using a portable condensation particle counter (CPC, model TSI 3007, 1–1000 nm particle size range) in the near field (NF, around 0.5–1 m far from the source). Regarding the chemical composition and morphology of the particles potentially released during the monitoring campaign, a Tygon tube (length 1 m) at 30 cm from the mouth of the worker was set to monitor particle release near the breathing zone. Moreover, two high flow peristaltic pumps (Casella, model APEX), containing a polycarbonate HEPA filter with a 37 mm diameter and a 0.4 µm pore size, were fixed on the lab coat of the worker settled at 30 cm from the mouth to collect particles in air during the monitoring campaign. Filters were then observed by scanning electron microscopy analysis using a field emission

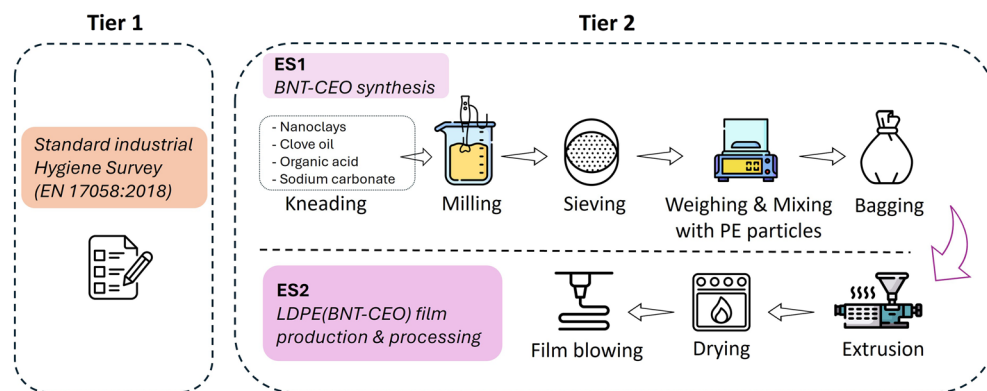


**Fig. 3** Schematic of the tiered methodology approach applied to assess the occupational safety and health (OSH) aspects of the BNT-CEO synthesis (ES1) and the LDPE(BNT-CEO) film production and processing (ES2).



scanning electron microscope, FESEM (Carl Zeiss Sigma NTS, Germany). Elemental analysis was performed by image analysis using FESEM coupled to an energy dispersive X-ray micro-analyser (EDS, mod. INCA).

Finally, according to the NanoGEM standard operation procedures (SOP) for assessing exposure to nanomaterials (Asbach *et al.*, 2014) and applied in Brunelli *et al.*, 2024, the criterion used to evaluate the results from tier 2 was the comparison of the particle concentration values obtained during the different activities monitored and the particle background concentration, by applying eqn (1) as follows:

$$C_{\text{net}} - C_{\text{bg}} > 3 \cdot S^2(\text{DBI}) \quad (1)$$

where  $C_{\text{net}}$  is the particle emission/exposure concentration,  $C_{\text{bg}}$  is the particle background concentration and  $S^2(\text{DBI})$  is the standard deviation of the particle background concentration. If  $C_{\text{net}} - C_{\text{bg}}$  is greater than  $3 \cdot S^2(\text{DBI})$ , the recorded particle concentration is considered statistically significant when compared to the background values. As a result, tier 3 assessment has to be performed to further evaluate the release of airborne nano-objects. In detail, tier 3 requires repeating the measurements performed in tier 2, along with the simultaneous collection of particles for off-line analysis, including mass or fiber concentration, particle morphology, and chemical composition. More details on this approach were reported in Brunelli *et al.*, 2024.

## 2.5 Food contact migration testing

**2.5.1 Pristine films.** According to the Regulation (EU) No 10/2011 on Plastic Materials and Articles, food contact material (FCM) migration testing was carried out by exposing LDPE and LDPE(BNT-CEO) films to different food simulants. Overall migration (OM) tests were performed with type A (EtOH 10% v/v, for hydrophilic food) and type D1 (EtOH 50% v/v, for food with a lipophilic character) food simulants. The standard establishes an OM limit of  $10 \text{ mg dm}^{-2}$  for general plastics meant to be used as food packaging. Both tests consisted of weighing  $1 \text{ dm}^2$  of each film and immersing it completely in 200 ml of food simulant for 10 days at  $40^\circ\text{C}$  in a closed container. Subsequently, the materials were dried in an oven at  $40^\circ\text{C}$  for 24 h and weighed. The difference in mass of each film before and after the test was then calculated. In addition to OM, a specific migration (SM) test for eugenol was conducted using LDPE films and polypropylene oxide (PPO, Tenax®), a food simulant (type E) complying with Regulation (EU) No 10/2011 for dry food. The SM limit was set at  $0.01 \text{ mg kg}^{-1}$ . PPO was purified *via* Soxhlet extraction with acetone (6 h), dried at  $80^\circ\text{C}$  overnight, and conditioned at  $160^\circ\text{C}$  (6 h). Circular LDPE films (6 cm diameter) were put in contact with 1 g of PPO in sealed, foiled covered glass plates and stored at  $60^\circ\text{C}$  for 10 days to simulate long-term, high temperature use.

After exposure, eugenol was extracted from the PPO using two 10 mL aliquots of HPLC-grade hexane with orbital

agitation. The combined extracts were filtered ( $3 \mu\text{m}$  Teflon) and analyzed *via* GC-MS to quantify the migrated eugenol. The test was performed in duplicate for reliability.

Besides these tests, further investigations not strictly required by Regulation No 10/2011 focused on: i) film modifications after a 10 day immersion test in simulant A (EtOH 10% v/v) by FT-IR and Raman spectroscopy; ii) potential release of fragments from both pristine and LDPE(BNT-CEO) films after the 10 day test in simulant A through a transmission electron microscope (TEM, JEOL JEM2010 200 kV) coupled with an electron dispersive X-ray spectrometer (EDX, X-Max 80, Oxford Instruments); iii) quantification of typical inorganic elements that could migrate from the LDPE(BNT-CEO) film (*i.e.*, Al, Mg, Na and Si) by analyzing the whole liquid sample through inductively coupled plasma-optical emission spectroscopy (ICP-OES, Thermo Jarrell Ash IRIS Advantage). The calibration curve was prepared using a multi standard solution within the concentration range of  $20\text{--}500 \text{ mg L}^{-1}$ , ensuring at least five calibration points within its linear response. The wavelengths used were as follows: 396.153 nm for Al, 280.271 nm for Mg, 589.592 nm for Na and 251.611 nm for Si.

For fragment release investigation, 1 mL aliquot of the washing water sample was deposited on a C-coated 200 mesh Cu grid before imaging.

**2.5.2 Accelerated aging of films.** Considering the potential long storage of food packaging under extreme environmental conditions, accelerated aging of both LDPE and LDPE(BNT-CEO) films was performed by using a xenon Q-SUN Xe-3 climatic chamber. This experiment followed the ISO 4892-2/2013 method (Plastics – Methods of exposure to laboratory light sources – Part 2: Xenon-arc lamps) which has been used already by different authors for nano-based plastic material weathering.<sup>50–52</sup> Specimens in Fig. S5 were aged up to 100 h with cycles of 102 min UV + 18 min water spray intervals,  $60 \text{ W m}^{-2}$  UV intensity and 300–400 nm as the wavelength range of emitted light. The chemical identity of the pristine samples after the 10 day test immersion was compared to that of the aged ones after the same immersion step by FTIR and  $\mu$ Raman spectroscopy. Then, the overall migration from aged samples into food simulant A was evaluated using the procedure previously described, in agreement with the Regulation (EU) No 10/2011 on Plastic Materials and Articles (*i.e.*, 10 days at  $40^\circ\text{C}$  exposed to simulant A in a closed container, drying in an oven at  $40^\circ\text{C}$  for 24 h and weighing). Afterwards, 1 mL of simulant A was deposited on a C-coated 200 mesh Cu grid and analyzed by TEM-EDX to investigate the presence of any potential fragment (*i.e.*, degraded LDPE matrix with embedded BNT-CEO or agglomerated BNT-CEO with some degradation debris attached or occasionally free BNT-CEO) from the accelerated weathered LDPE(BNT-CEO) films. The potential release of any inorganic element which could be ascribed to the nanoclays was investigated by ICP-OES spectroscopy. In detail, simulant A was centrifuged at 11139 rcf for 10 min (Centrifuge 5910 R, Eppendorf SE) and 20 ml of supernatant



were analyzed. Lastly, the remaining food simulant was lyophilized, and the remaining solid material was studied via FT-IR and  $\mu$ Raman spectroscopy.

### 3. Results and discussion

#### 3.1 Preliminary insect barrier performance

Before starting the SSbD assessment, a preliminary insect barrier test was conducted, since information on the materials' functionality with respect to the benchmark already on the market is a prerequisite for any further product development.

The preliminary barrier performance assay results are reported in Table S1. According to ANOVA followed by Tukey's HSD test ( $\alpha = 0.05$ ), two statistically distinct groups were identified ((a) and (b)), when comparing the number of *T. castaneum* individuals found inside the sachets. All LDPE(BNT-CEO) films, regardless of concentration (1%, 2%, or 5% w/w) or microperforation, clustered in the same group (a), with very low insect penetration (0.00–2.10 per replicate). In contrast, the control LDPE film without an additive formed a separate group (b), with a significantly higher number of penetration (13.70 per replicate), which was statistically different from the active films ( $p < 0.05$ ). This assay showed the substantial protective effect of BNT-CEO, as its presence consistently reduced pest intrusion compared to pristine LDPE (selected as the control). Notably, this effect was observed even with the lowest concentration (1 wt%), but no dose-dependent trend was found. Based on the data in Table S1, the 2 wt% concentration of BNT-CEO in the polymer was identified as the most suitable for further assessment.

#### 3.2 Hazard assessment of the BNT-CEO

##### 3.2.1 Advanced material physicochemical characterization.

A preliminary investigation of BNT powder was performed to obtain some basic information on its characteristics. In detail, the specific surface area and total pore volume were  $82 \text{ m}^2 \text{ g}^{-1}$  and  $0.16 \text{ cm}^3 \text{ g}^{-1}$ , respectively. The adsorption capacity expressed as cation exchange capacity was 86 meq (100 g) $^{-1}$  and the carbon content was 1.8%. The mineral composition of BNT by means of XRD (Fig. S6) showed montmorillonite as the main component (82%), with also the presence of opal (12%), feldspar (3%), plagioclase (1%) and calcite (2%).

Afterwards, the encapsulation of CEO within BNT was studied by FE-SEM, FT-IR and TGA. The FE-SEM images of BNT and BNT loaded with CEO (BNT-CEO) powders are displayed in Fig. S7. A higher agglomeration pattern and the appearance of a rougher shape on the edges of BNT-CEO in comparison with the raw BNT were observed. The FT-IR spectra of BNT, CEO and BNT-CEO are displayed in Fig. S7c. The encapsulation of CEO into BNT powder was confirmed by the appearance of some of the characteristic bands of CEO in the BNT-CEO, *i.e.*, at  $2928 \text{ cm}^{-1}$  ( $-\text{CH}$  stretching), at  $1637$  and  $1608 \text{ cm}^{-1}$  ( $-\text{C}=\text{C}-$  valence stretching) and at  $1515 \text{ cm}^{-1}$

( $-\text{C}-\text{C}-$  aromatic). The comparison of weight loss through TGA between BNT and BNT-CEO in Fig. S7d showed a 16.5% difference above  $200^\circ\text{C}$ , highlighting the presence of clove oil in the BNT-CEO sample.

Besides the evaluation of the intrinsic characteristics of both BNT and BNT-CEO, also the potential release of eugenol from BNT-CEO was determined by performing UV-vis spectroscopy analysis at different time points, along a weathering experiment. Measurements have been first conducted at room temperature and then after increasing the temperature to  $80^\circ\text{C}$ . The results displayed in Fig. S8 showed negligible eugenol release at RT and only around 5% at  $80^\circ\text{C}$ , throughout the 30 days of testing.

Embedding of BNT-CEO to LDPE films was investigated by means of FT-IR and  $\mu$ Raman spectroscopy, and the results are displayed in Fig. S9. The characteristic bands observed from the FT-IR spectrum of LDPE are at  $2914 \text{ cm}^{-1}$  ( $-\text{CH}_2-$  asymmetric),  $2847 \text{ cm}^{-1}$  ( $-\text{CH}_2-$  symmetric),<sup>53</sup>  $1465 \text{ cm}^{-1}$  (deformation vibration band of  $-\text{CH}_2-$ ) and  $1444 \text{ cm}^{-1}$  ( $-\text{CH}_2-$  pending mode).<sup>50,54</sup> The same signals were also observed for the LDPE(BNT-CEO). With regard to the analysis by  $\mu$ Raman spectroscopy, the spectra of LDPE and LDPE(BNT-CEO) films were comparable and in good agreement with the literature,<sup>55–57</sup> with typical LDPE signals at  $2882$  and  $2848 \text{ cm}^{-1}$  (C-H methyl stretching vibration),  $2721 \text{ cm}^{-1}$  (overtone  $-\text{CH}_2$ ),  $1440 \text{ cm}^{-1}$  ( $-\text{CH}_2$  bending),  $1295 \text{ cm}^{-1}$  ( $-\text{CH}_2$  twisting), and  $1129 \text{ cm}^{-1}$  and  $1063 \text{ cm}^{-1}$  (C-C stretching). The presence of BNT-CEO was confirmed by the images obtained through TEM and Raman microscopy (Fig. S10).

Furthermore, the results of eugenol loss from the LDPE(BNT-CEO) films exposed to air over 12 months under controlled conditions are displayed in Fig. 4. The maximum percentage of eugenol released was 33% after 12 months of aging.

**3.2.2 Hazard property evaluation of the BNT-CEO precursors.** Following the approach published in Brunelli *et al.*, 2024 and in accordance with the EU-JRC SSbD

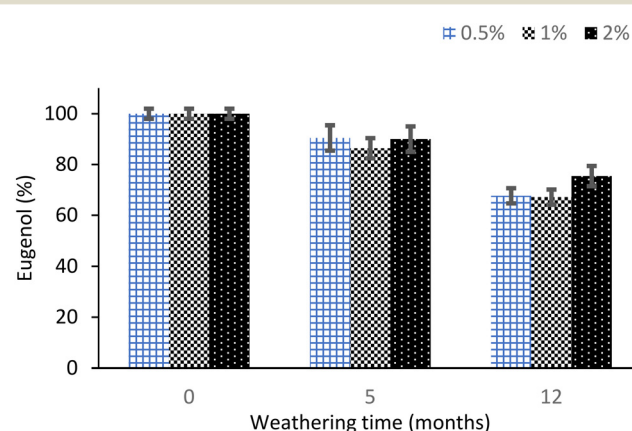


**Fig. 4** Amount of eugenol (%) still embedded in the LDPE(BNT-CEO) films after 0, 5 and 12 months of aging. The results are expressed as the mean  $\pm$  SD of measurements from three independent films.



framework, the hazard evaluation of the chemicals used for the synthesis of BNT-CEO was conducted. Substances were evaluated according to the criteria outlined in the EU-JRC SSBd framework (*i.e.*, criterion H1 = most harmful substances, criterion H2 = substances of concern, criterion H3 = other hazard properties), based on hazard classes and categories identified by means of CLP and REACH regulations. According to Regulation (EC) No. 1272/2008, BNT powder is classified as a non-hazardous substance. However, the SDS of CEO lists acute toxicity (category 4, H302), skin sensitization (sub-category 1B, H317), and eye irritation (category 2, H319). The same risk phrase for eye irritation (category 2, H319) also applies to both anhydrous sodium carbonate and citric acid. Additionally, citric acid poses a risk of respiratory irritation (category 3, H335). As a result, the workflow followed for the hazard assessment of the chemicals used for the synthesis of BNT-CEO is displayed in Fig. 5.

Based on the criteria defined in the EU-JRC SSBd framework, all the chemicals evaluated passed the criteria H1 and H2 but not the H3. Therefore, according to the evaluation system proposed by the SSBd framework, the chemicals used for the synthesis of BNT-CEO belong to level 2.

**3.2.3 In vitro toxicological evaluation of the BNT-CEO.** BNT-CEO mixed with xanthan gum (BNT-CEO-XG) was used for the *in vitro* toxicity testing given its increased dispersion stability required to run the CBMN assay. XG alone was also included in the evaluation, together with the other components comprising the BNT-CEO; the individual constituents have been tested at a concentration corresponding to their ratio within the highest dose of BNT-

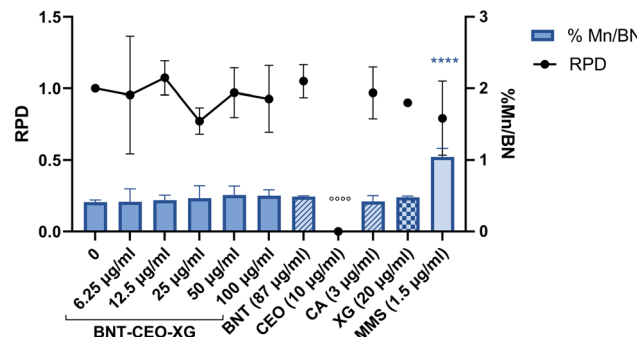


**Fig. 6** Cytotoxicity (RPD) and genotoxicity (% Mn/BN) of BNT-CEO-XG and its single components (BNT = bentonite, CEO = clove essential oil, CA = citric acid, XG = xanthan gum).  $N = 3$ , MMS (methyl methane sulfonate) was used as a positive control. Statistical analysis *via* ordinary one-way ANOVA:  $^* p < 0.005$ ,  $^{**} p < 0.001$ ,  $^{****} p < 0.0001$ .

CEO investigated. Statistical analysis was performed using the ANOVA test.

Despite the high toxicity of CEO, the BNT-CEO-XG did not significantly reduce cell survival (Fig. 6). The figure also shows that the addition of XG does not modify the toxicological profile of BNT-CEO. The micronucleus frequency did not change substantially compared to the untreated control, indicating that no genotoxic response was induced.

### 3.3 Occupational exposure assessment

**3.3.1 Dustiness.** The data obtained from dustiness measurements revealed  $3037 \pm 1889$  particles per  $\text{cm}^3$  for BNT (corresponding to a total amount of  $\sim 20700$  particles),

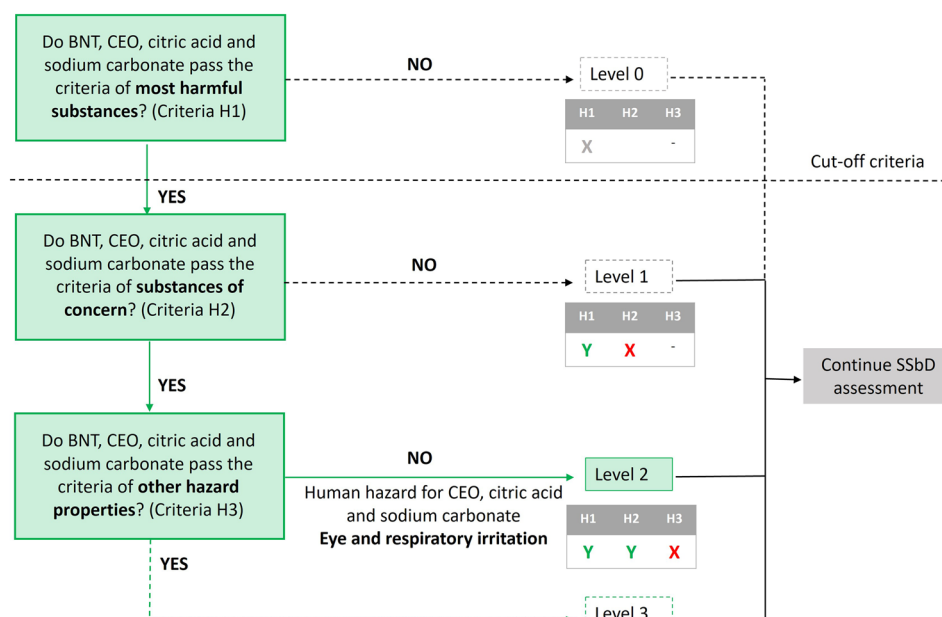


**Fig. 5** Workflow of the hazard assessment of the individual chemicals used for the BNT-CEO synthesis, according to step 1 of the EU-JRC SSBd framework. The pathway followed is represented by solid lines and green rectangles.



which decreased to  $52 \pm 5$  particles per  $\text{cm}^3$  for BNT-CEO (corresponding to a total amount of  $\sim 600$  particles). This might indicate a general decrease of the particle number per  $\text{cm}^3$  due to the encapsulation process, in agreement with the higher agglomeration observed by TEM for BNT-CEO (Fig. S7b) with respect to BNT (Fig. S7a). Therefore, a potential decrease of exposure to the BNT-CEO with respect to pristine BNT can be hypothesized. In addition, dustiness measurements were also performed to assess if upon release in air, the resulting aerosol can be inhaled and have a likelihood to reach the lungs. The MMAD for both samples was  $< 1.5 \mu\text{m}$  (BNT:  $1.04 \mu\text{m}$  MMAD and geometric standard deviation (gsd) of 1.34; BNT-CEO:  $0.84 \mu\text{m}$  MMAD and gsd of 1.43), which implies that the materials can be inhaled, and a portion falls within the respirable fraction.

**3.3.2 NanoGEM three-tiered methodology.** The survey administered to identify the potential sources of particle emission during production and processing is included in the SI (Tables S2 and S3). The outcomes of the survey were used to guide the OSH assessment for both BNT-CEO synthesis (ES1) and LDPE(BNT-CEO) production and processing (ES2) by performing two different air monitoring campaigns, following the scheme displayed in Fig. 3. The data collected through a CPC for both the ES investigated are summarized in Tables S3 and S4 and Fig. 7, displaying the particle number concentration (particle number per  $\text{cm}^3$ ) vs. time. Background CPC data showed a mean of  $10\,738 \pm 363$  particles per  $\text{cm}^3$  for ES1 (Fig. 7a) and  $13\,153 \pm 1001$  particles per  $\text{cm}^3$  for ES2 (Fig. 7b). With regard to ES1, CPC readings during the selected activities showed an almost steady particle concentration over time, except only when BNT-CEO powder leaked out during bagging, reaching 11 986 particles per  $\text{cm}^3$ . For ES2, the occupational monitoring revealed a “particle release event” (around 42 000 particles per  $\text{cm}^3$ ), attributed to the handling of the LDPE(BNT-CEO) in the powder form added to the extruder inlet. Another peak of particle release was observed after 15 minutes from the

previous one, with a particle concentration reaching up to  $\sim 25\,000$  particles per  $\text{cm}^3$ . This might be due to overheating of the first extruded mixture.

The data recorded for pellet drying and film blowing activities were almost constant and similar to the background levels over the monitoring campaign, except for a peak of 25 000 particles per  $\text{cm}^3$  detected when the oven's door was opened.

SEM-EDX images of samples collected during the occupational monitoring campaign are reported in Fig. S11–S14. Typical airborne particles were identified, showing single or multiple clay leaflets in the 1–10  $\mu\text{m}$ -size range. Regardless of the ES considered, almost all EDX spectra showed the presence of carbon and oxygen, which could be attributed to the polycarbonate substrate. Some spectra revealed the presence of Si signals, with less frequent signals ascribable to Al, Ca, Fe, K, Mg and Na. This could indicate potential exposure to elements characteristic of BNT.

In summary, while the particle concentration recorded remained relatively low and constant over the occupational monitoring campaign, SEM images indicated potential exposure to particles during both the BNT-CEO synthesis and the LDPE(BNT-CEO) processing and production.

In order to mitigate exposure, the use of additional personal protective equipment (PPE) besides the standard fume hood must be implemented. Furthermore, the adoption of a hopper system for pouring the material into the extruder is strongly recommended. This measure will significantly reduce the energy input to the particles, thereby preventing particle release events of around 42 000 particles per  $\text{cm}^3$  like the one previously observed.

### 3.4 Food contact material migration testing

**3.4.1 Food contact material migration testing (FCM) from pristine LDPE(BNT-CEO) films.** FCM migration testing was performed on both pristine films (food simulants A and E)

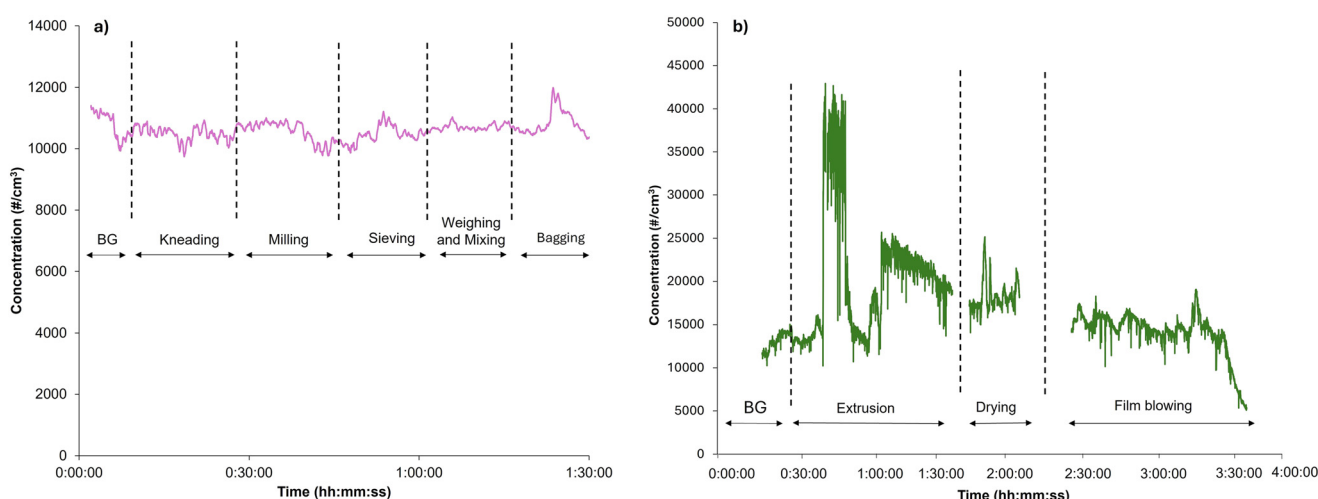


Fig. 7 Particle number concentration during a) BNT-CEO synthesis (ES1) and b) LDPE(BNT-CEO) production and processing (ES2).



and aged films (food simulant A). The results related to pristine films in food simulant type A revealed that the overall migration of substances per  $\text{dm}^2$  of surface area of the plastic material reached  $0.6 \pm 0.1 \text{ mg dm}^{-2}$  for both LDPE and LDPE(BNT-CEO) films. These values were always below the limit of  $10 \text{ mg dm}^{-2}$ , set by the Regulation (EU) No 10/2011 on Plastic Materials and Articles.

In the specific migration test using food simulant E, a significant reduction in eugenol release was observed from the LDPE(BNT-CEO) film. Eugenol migration from the LDPE(BNT-CEO) reached  $2 \pm 0.1 \text{ mg kg}^{-1}$ , while  $5 \pm 0.1 \text{ mg kg}^{-1}$  was detected from the virgin LDPE. A notable finding was the high eugenol value of  $10 \pm 1 \text{ mg kg}^{-1}$  in the blank sample, suggesting the presence of background contamination.

While the (LDPE)BNT-CEO film effectively reduced eugenol release, both films failed to meet the  $0.01 \text{ mg kg}^{-1}$  "not detectable" limit set by EU Regulation No 10/2011. This suggests that although the hybrid matrix immobilizes eugenol, further optimization of the encapsulation strategy, such as adjusting the essential oil loading or using additional barrier layers, is necessary to achieve regulatory compliance while maintaining functionality.

In addition to the overall and specific migration tests, the release of potential fragments from the films and the presence of elements from the BNT-CEO were investigated in food simulant A by TEM-EDX and ICP-OES. TEM-EDX analysis revealed the presence of very few particles, mostly agglomerated (Fig. 8). EDX analysis in Fig. S15 showed agglomerates with the presence of Si that could be the only element ascribed to the presence of BNT-CEO but no other inorganic elements characteristic of the nanoclays (e.g., Al) were detected. The results from ICP-OES are reported in the next section, comparing the results between pristine and aged films.

**3.4.2 Accelerated aging of films, overall migration and fragment release investigation.** Even if the Regulation (EU) No 10/2011 on Plastic Materials and Articles does not include

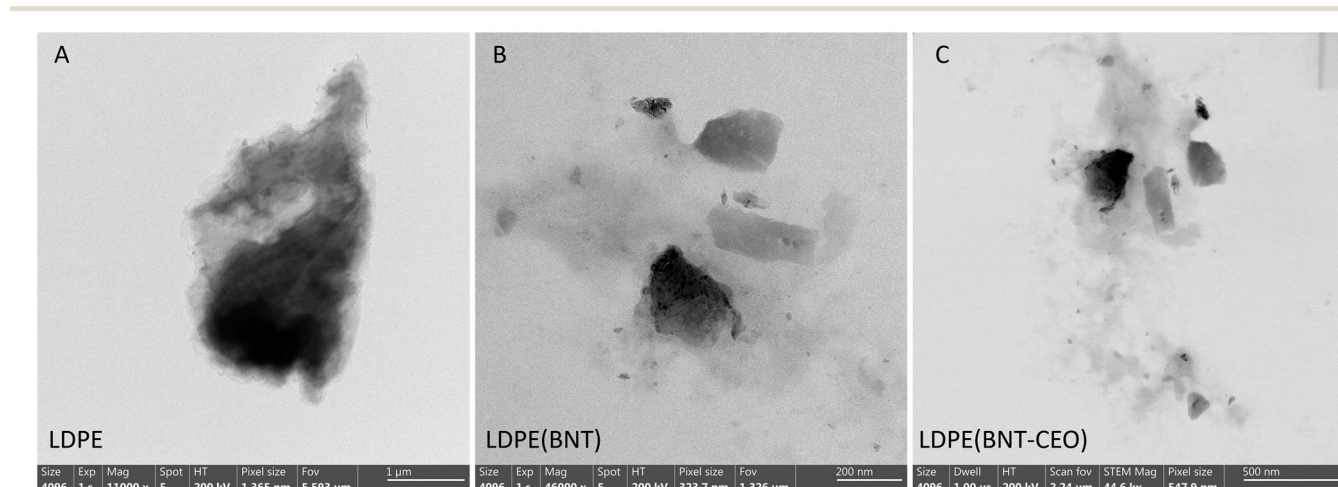


Fig. 8 Typical TEM images of A) LDPE, B) LDPE(BNT) and C) LDPE(BNT-CEO) samples.

any constraints or threshold to be complied with for an aged material, the same approach used for pristine films was also adopted for the aged ones. The only difference was a further investigation of the lyophilized samples through FT-IR and Raman spectroscopy.

After accelerated aging, overall migration (OM) was below  $0.01 \text{ mg per dm}^2$  of the film, for both LDPE and LDPE(BNT-CEO) after accelerated aging. Moreover, FT-IR and  $\mu$ Raman analyses were carried out on both LDPE and LDPE(BNT-CEO) films after the 10 day immersion, and the corresponding spectra, together with those acquired on pristine materials, are displayed in Fig. S16. The characteristic bands observed for the aged samples were the same as for the pristine ones previously described. Indeed, no peak shifting was observed, and only small intensity variations have been detected for the aged samples with respect to the pristine samples. The fragments from aged samples observed by TEM-EDX are displayed in Fig. S17, indicating a  $\mu\text{m}$ -sized dimension and a C-based composition combined with the presence of several inorganic elements (e.g., Ca, Cl, Fe, K, N, Na, O, S, and Si). The concentration values of the inorganic elements investigated by ICP-OES, taking into account that the only threshold for non-aged materials in Annex II, Table 1 of Regulation 1245/2020 is for Al ( $\leq 1 \text{ mg kg}^{-1}$  food simulant), were not of significant concern, with Al  $< 0.005 \text{ mg kg}^{-1}$ , Na  $< 0.1 \text{ mg kg}^{-1}$  and Si  $< 0.2 \text{ mg kg}^{-1}$  (Fig. S18).

Based on these considerations, the LDPE(BNT-CEO) film complies with the FCM regulation on plastic materials and articles.

Lastly, lyophilized samples were investigated by FT-IR and  $\mu$ Raman spectroscopy against the blank sample (food simulant A only, i.e., 10% EtOH). The results in Fig. S19 suggest that the characteristic bands observed for aged LDPE and aged LDPE(BNT-CEO) after freeze-drying are similar to those recorded for the blank sample. This confirms that only some impurities were detected as fragments, but no indication of the presence of LDPE or LDPE(BNT-CEO) fragments was observed.



### 3.5 Advanced material safety assessment – summary

The early innovation stage assessment of the safety dimension for BNT-CEO embedded in LDPE food packaging was performed by collecting and merging information from the literature and from experimental data specifically generated for this material.

The physicochemical characterization of the final material proved the effectiveness of the MCNM synthesis procedure. In summary, a) an effective loading of CEO onto BNT, with a negligible release of eugenol over time at RT and only around 5% at 80 °C, was revealed; b) a controlled release of eugenol from the LDPE(BNT-CEO) film was achieved, reaching a 33% maximum release after 12 month exposure to air.

For the hazard assessment, the safety data sheets of the advanced MCNM constituents revealed that citric acid and sodium carbonate were the only hazardous components due to them being potential eye and respiratory irritants. The *in vitro* cytotoxicity and genotoxicity assays performed demonstrated no significant reduction of cell viability and no genotoxicity induced by the MCNM.

Moving from hazard to occupational exposure assessment, the results of the preliminary dustiness testing suggested a decrease of BNT-CEO exposure with respect to pristine BNT. This indicates that the encapsulation process successfully limits the release of particles, even if the MMAD of both materials indicated potential for inhalation, since a fraction of particles fell within the respirable fraction. The NanoGEM three-tiered methodology applied for the monitoring indicated workers' potential exposure to particles containing typical elements of BNT, during both MCNM synthesis (ES1) and LDPE(BNT-CEO) production and processing (ES2). Given these results, we consider essential the implementation of appropriate personal protective equipment (PPE) and the use of fume hoods in both exposure scenarios to reduce the occupational exposure to hazardous materials.

Lastly, the safety assessment of the advanced MCNM focused on consumer exposure assessment, involving FCM tests on pristine as well as on accelerated aged LDPE(BNT-CEO) films.

The results suggested that the AdMa does not pose any regulatory concern since:

- I. no significant surface modifications were observed after 10 day immersion in food simulant A;
- II. no significant release of substances ascribable to the BNT-CEO was recorded;
- III. OM values were always below the threshold limit set by the Regulation (EU) No 10/2011 on Plastic Materials and Articles;
- IV. no fragment release ascribable to the LDPE(BNT-CEO) films was detected.

Considering the selected scenarios, the innovative LDPE(BNT-CEO) film investigated through this study did not raise significant safety issues towards workers and potential consumers. The environmental safety aspects related to the BNT-CEO case study were recently investigated on

representative environmental models (*i.e.*, lettuce, *D. magna*, algae) by Brinkmann *et al.*, 2025.<sup>58</sup>

## 4. General remarks and conclusions

Traditional FCMs often include a variety of either synthetic or natural substances that may raise concerns regarding their durability and potential (eco)toxicological effects.

To overcome these challenges, new technologies and/or materials are needed, which come as well with safety and sustainability aspects. Building upon the work of Pizzol *et al.* (2023),<sup>36</sup> this study aims at helping the advancement of the early consideration of safety aspects during the development of an innovative LDPE-based food packaging material, in accordance with the pre-market safety assessment principles outlined in the EU-JRC SSbD framework.

Our approach identified only one critical safety aspect within the overall assessment, which was mitigated by recommending the implementation of additional PPEs.

The methodological approach proposed was designed to be general and flexible to ensure alignment with the EU-JRC SSbD framework. Its ability to gather information and highlight potential issues very early in product development can make it suitable for a broad applicability across various industrial sectors. For instance, this methodology was first implemented by Brunelli *et al.*, 2024, to assess the safety-by-design of an innovative material used in construction. Regardless of the specific sector, this approach helped to streamline the overall assessment – ranging from the physicochemical characterization of complex materials to the assessment of worker and consumer exposure – thereby boosting thorough innovation and commercialization of products.

This food packaging case study can therefore serve as a key (safety) pillar intended to guide future efforts toward early SSbD assessments for different types of AdMas, in alignment with the Green Deal ambition of phasing out harmful substances from the EU market. It also serves as a reference for the various actors and stakeholders – including producers, experts in food processing and packaging, retailers and distributors, as well as consumers – who are involved in the product value chain and are interested in applying this methodology.

Finally, the overall results of this safety assessment will be integrated with sustainability outcomes, and the combined information will be ultimately included in the freely accessible web-based SUNSHINE e-infrastructure (<https://www.sunshine.greendecision.eu/sign-in?origin=/sunshine>), a digital tool for SSbD decision-making specifically designed for industry.

## Author contributions

Conceptualization: A. Brunelli, E. Badetti; methodology: A. Brunelli, E. Badetti, D. Hristozov; formal analysis and



investigation: A. Brunelli, E. Badetti, A. Serrano-Lotina, M. A. Bañares, V. Alcolea-Rodriguez, M. Blosi, A. Costa, S. Ortelli, C. Fito, E. G. Fernandez, J. S. Hermosilla, F. Murphy, V. Stone, J. Balbuena, J. M. L. Cormano; writing – original draft preparation: A. Brunelli, E. Badetti, D. Hristozov, A. Serrano-Lotina, M. A. Bañares, H. Rauscher, F. Murphy, V. Stone, C. Fito, E. G. Fernandez, J. S. Hermosilla; writing – review and editing: A. Brunelli, E. Badetti, A. Serrano-Lotina, M. A. Bañares, V. Alcolea-Rodriguez, M. Blosi, A. Costa, S. Ortelli, W. Peijnenburg, C. Fito, E. G. Fernandez, J. S. Hermosilla, L. G. Soeteman-Hernández, I. Garmendia Aguirre, H. Rauscher, F. Murphy, V. Stone, L. Pizzol; funding acquisition: A. Brunelli, E. Badetti, D. Hristozov, A. Marcomini; supervision: A. Brunelli, E. Badetti, A. Marcomini.

## Conflicts of interest

There are no conflicts to declare.

## Data availability

The authors confirm that the data supporting the findings of this study are available within the article [and/or its SI]. Supplementary information is available. See DOI: <https://doi.org/10.1039/d5en00435g>.

## Acknowledgements

This work was performed in the frame of the European Union's Horizon 2020 research and innovation programme under the SUNSHINE (Safe and Sustainable Design for Advanced Materials) project (G.A. No. 952924) and it was supported by the DoE 2023-2027 (MUR, AIS.DIP. ECCELLENZA2023\_27.FF project). We are grateful to Rob Vandebriel (RIVM) for his efforts for and contribution to the H2020 SUNSHINE *in vitro* work. Icons in the manuscript were downloaded from <https://www.flaticon.com>.

## References

- 1 M. M. Aung and Y. S. Chang, Traceability in a food supply chain: Safety and quality perspectives, *Food Control*, 2014, **39**, 172–184.
- 2 A. N. Mafe, G. I. Edo, R. S. Makia, O. A. Joshua, P. O. Akpoghelie and T. S. Gaaz, *et al.*, A review on food spoilage mechanisms, food borne diseases and commercial aspects of food preservation and processing, *Food Chem. Adv.*, 2024, **5**, 100852.
- 3 S. Sala, V. De Laurentiis, E. S. Mengual, Food consumption and waste: environmental impacts from a supply chain perspective. European Commission, 2023.
- 4 EFSA and ECDC (European Food Safety Authority and European Centre for Disease Prevention and Control), The European Union One Health 2022 Zoonoses Report, *EFSA J.*, 2023, **21**(12), e8442.
- 5 European Commission, Regulation (EC) No 1935/2004 of the European Parliament and of the council of 27 October 2004 on materials and articles intended to come into contact with food and repealing Directives 80/590/EEC and 89/109/EEC. Official Journal of the European Union, 2004, Available from: <https://eur-lex.europa.eu/LexUriServ/LexUriServ.do?uri=OJ:L:2004:338:0004:0017:en:PDF>.
- 6 S. Rossi, S. Gemma, F. Borghini, M. Perini, S. Butini and G. Carullo, *et al.*, Agri-food traceability today: Advancing innovation towards efficiency, sustainability, ethical sourcing, and safety in food supply chains, *Trends Food Sci. Technol.*, 2025, **163**, 105154.
- 7 European Commission, Communication from the Commission: The European Green Deal, 2019, Available from: chrome-extension://efaidnbmnnibpcajpcglclefindmkaj/[https://eur-lex.europa.eu/resource.html?uri=cellar:b828d165-1c22-11ea-8c1f-01aa75ed71a1.0002.02/DOC\\_1&format=PDF](https://eur-lex.europa.eu/resource.html?uri=cellar:b828d165-1c22-11ea-8c1f-01aa75ed71a1.0002.02/DOC_1&format=PDF).
- 8 J. Muncke, A. M. Andersson, T. Backhaus, J. M. Boucher, B. Carney Almroth and A. Castillo Castillo, *et al.*, Impacts of food contact chemicals on human health: a consensus statement, *Environ. Health*, 2020, **19**(1), 25.
- 9 K. Marsh and B. Bugusu, Food packaging–roles, materials, and environmental issues, *J. Food Sci.*, 2007, **72**(3), R39–R55.
- 10 G. Robertson, *Food Packaging - Principles and Practice*, 3rd edn, 2012, p. 733, DOI: [10.1201/b21347](https://doi.org/10.1201/b21347).
- 11 V. Stejskal, J. Hubert, R. Aulicky and Z. Kucerova, Overview of present and past and pest-associated risks in stored food and feed products: European perspective, *J. Stored Prod. Res.*, 2015, **64**, 122–132.
- 12 G. Robertson, *Food Packaging: Principles and Practice*. CRC Press, Boca Raton, FL, USA, 2nd edn, 2005, p. 550.
- 13 E. O. Essig, W. M. Hoskins, E. G. Linsley, A. E. Micrelbacher and R. F. Smith, A Report on the Penetration of Packaging Materials by Insects, *J. Econ. Entomol.*, 1943, **36**(6), 822–829.
- 14 P. D. Gerhardt and D. L. Lindgren, Penetration of Additional Packaging Films by Common Stored-Product Insects1, *J. Econ. Entomol.*, 1955, **48**(1), 108–109.
- 15 FAO, Food and Agriculture Organization of the United Nations, 2024, Available from: <https://www.fao.org/plant-production-protection/en>, visited on 28.03.2024.
- 16 C. E. Realini and B. Marcos, Active and intelligent packaging systems for a modern society, *Meat Sci.*, 2014, **98**(3), 404–419.
- 17 X. Hou, P. Fields and W. Taylor, The effect of repellents on penetration into packaging by stored-product insects, *J. Stored Prod. Res.*, 2004, **40**(1), 47–54.
- 18 F. Licciardello, G. Muratore, P. Suma, A. Russo and C. Nerín, Effectiveness of a novel insect-repellent food packaging incorporating essential oils against the red flour beetle (*Tribolium castaneum*), *Innovative Food Sci. Emerging Technol.*, 2013, **19**, 173–180.
- 19 M. A. Mullen, S. V. Mowery, Chapter 6 - Insect-Resistant Packaging, in *Insect Management for Food Storage and Processing*, ed. J. W. Heaps, AACC International Press, 2nd edn, 2006, pp. 35–38. Available from: <https://www.sciencedirect.com/science/article/pii/B9781891127465500118>.



20 M. Alonso-Gato, G. Astray, J. C. Mejuto and J. Simal-Gandara, Essential Oils as Antimicrobials in Crop Protection, *Antibiotics*, 2021, **10**(1), 34.

21 L. Catani, E. Grassi, A. Cocozza di Montanara, L. Guidi, R. Sandulli and B. Manachini, *et al.*, Essential oils and their applications in agriculture and agricultural products: A literature analysis through VOSviewer, *Biocatal. Agric. Biotechnol.*, 2022, **45**, 102502.

22 CORDIS, Results Pack on advanced materials - A thematic collection of innovative EU-funded research results, 2023.

23 S. A. O. Adeyeye and T. J. Ashaolu, Applications of nanomaterials in food packaging: A review, *J. Food Process Eng.*, 2021, **44**(7), e13708.

24 G. S. Germinara, A. Conte, L. Lecce, A. Di Palma and M. A. Del Nobile, Propionic acid in bio-based packaging to prevent *Sitophilus granarius* (L.) (Coleoptera, Dryophthoridae) infestation in cereal products, *Innovative Food Sci. Emerging Technol.*, 2010, **11**(3), 498–502.

25 T. Hirvikorpi, M. Vähä-Nissi, T. Mustonen, E. Iiskola and M. Karppinen, Atomic layer deposited aluminum oxide barrier coatings for packaging materials, *Thin Solid Films*, 2010, **518**(10), 2654–2658.

26 A. M. Marsin, I. I. Muhamad, S. N. S. Anis, N. A. M. Lazim, L. W. Ching and N. H. Dolhaji, Essential oils as insect repellent agents in food packaging: a review, *Eur. Food Res. Technol.*, 2020, **246**(8), 1519–1532.

27 P. Chaudhary, F. Fatima and A. Kumar, Relevance of Nanomaterials in Food Packaging and its Advanced Future Prospects, *J. Inorg. Organomet. Polym. Mater.*, 2020, **30**(12), 5180–5192.

28 A. Ashfaq, N. Khursheed, S. Fatima, Z. Anjum and K. Younis, Application of nanotechnology in food packaging: Pros and Cons, *J. Agric. Food Res.*, 2022, **7**, 100270.

29 EFSA Scientific Committee, S. More, V. Bampidis, D. Benford, C. Bragard, T. Halldorsson, A. Hernández-Jerez, S. Hougaard Bennekou, K. Koutsoumanis, C. Lambré, K. Machera, H. Naegeli, S. Nielsen, J. Schlatter, D. Schrenk, V. Silano, D. Turck, M. Younes, J. Castenmiller, Q. Chaudhry, F. Cubadda, R. Franz, D. Gott, J. Mast, A. Mortensen, A. G. Oomen, S. Weigel, E. Barthelemy, A. Rincon, J. Tarazona and R. Schoonjans, Guidance on risk assessment of nanomaterials to be applied in the food and feed chain: human and animal health, *EFSA J.*, 2021, **19**(8), 6768.

30 M. Kaur, S. Sharma and A. Kalia, Nano-laminated clay-essential oil composite formulations: Key mechanistic antibacterial processes and in vitro antibiofilm activity, *J. Drug Delivery Sci. Technol.*, 2025, **104**, 106447.

31 M. Alboofetileh, M. Rezaei, H. Hosseini and M. Abdollahi, Antimicrobial activity of alginate/clay nanocomposite films enriched with essential oils against three common foodborne pathogens, *Food Control*, 2014, **36**(1), 1–7.

32 L. H. de Oliveira, P. Trigueiro, J. S. N. Souza, M. S. de Carvalho, J. A. Osajima and E. C. da Silva-Filho, *et al.*, Montmorillonite with essential oils as antimicrobial agents, packaging, repellents, and insecticides: an overview, *Colloids Surf. B*, 2022, **209**, 112186.

33 A. Giannakas, I. Tsagkalias, D. S. Achilias and A. Ladavos, A novel method for the preparation of inorganic and organo-modified montmorillonite essential oil hybrids, *Appl. Clay Sci.*, 2017, **146**, 362–370.

34 M. G. M. Nguemtchouin, M. B. Ngassoum, P. Chalier, R. Kamga, L. S. T. Ngamo and M. Cretin, Ocimum gratissimum essential oil and modified montmorillonite clay, a means of controlling insect pests in stored products, *J. Stored Prod. Res.*, 2013, **52**, 57–62.

35 C. Caldeira, R. Farcal, A. I. Garmendia, L. Mancini, D. Tosches and A. Amelio, *et al.*, Safe and sustainable by design chemicals and materials - Framework for the definition of criteria and evaluation procedure for chemicals and materials. JRC Publications Repository, 2022, Available from: <https://publications.jrc.ec.europa.eu/repository/handle/JRC128591>.

36 L. Pizzol, A. Livieri, B. Salieri, L. Farcal, L. G. Soeteman-Hernández and H. Rauscher, *et al.*, Screening level approach to support companies in making safe and sustainable by design decisions at the early stages of innovation, *Clean. Environ. Syst.*, 2023, **10**, 100132.

37 C. Salgado, J. F. F. Lozano, J. J. Reinosa and D. A. Domínguez, Functional clays with controlled release of natural additives. 2024.

38 B. Singh and N. Sharma, Mechanistic implications of plastic degradation, *Polym. Degrad. Stab.*, 2008, **93**, 561–584.

39 M. D. Pointer, M. J. G. Gage and L. G. Spurgin, Tribolium beetles as a model system in evolution and ecology, *Heredity*, 2021, **126**(6), 869–883.

40 OECD, Study Report and Preliminary Guidance on the Adaptation of the In Vitro micronucleus assay (OECD TG 487) for Testing of Manufactured Nanomaterials - Series on Testing and Assessment No. 359. Organisation for Economic Co-Operation and Development - ENV/CBC/MONO(2022)15, 2022.

41 C. Asbach, T. A. J. Kuhlbusch, H. Kaminiski, B. Stahlmecke, S. Plitzo and U. Gotz, *et al.*, Standard Operation Procedures For assessing exposure to nanomaterials, following a tiered approach. 2012.

42 BAuA, BG RCI, IFA, IUTA, TUD and VCI, Tiered Approach to an Exposure Measurement and Assessment of Nanoscale Aerosols Released from Engineered Nanomaterials in Workplace Operations. 2011.

43 M. Methner, L. Hodson and C. Geraci, Nanoparticle emission assessment technique (NEAT) for the identification and measurement of potential inhalation exposure to engineered nanomaterials–part A, *J. Occup. Environ. Hyg.*, 2010, **7**(3), 127–132.

44 OECD, OECD Physical-chemical decision framework to inform decisions for risk assessment of manufactured nanomaterials. Organisation for Economic Co-Operation and Development, 2019.

45 OECD, Strategies, techniques and sampling protocols for determining the concentrations of manufactured nanomaterials in air at the workplace. ENV/JM/MONO(2017)30, 2017, Available from: [https://one.oecd.org/document/ENV/JM/MONO\(2017\)30/en/pdf](https://one.oecd.org/document/ENV/JM/MONO(2017)30/en/pdf).

46 A. Brunelli, A. Serrano-Lotina, M. A. Bañares, V. Alcolea-Rodriguez, M. Blosi and A. Costa, *et al.*, Safe-by-design assessment of an  $\text{SiO}_2@\text{ZnO}$  multi-component nanomaterial used in construction, *Environ. Sci.: Nano*, 2025, **12**, 762–776.

47 European Committee for Standardization, EN17058:2018 - Workplace exposure - Assessment of exposure by inhalation of nano-objects and their aggregates and agglomerates, European Standards, 2018.

48 European Chemicals Agency, An illustrative example of the exposure scenarios to be annexed to the safety data sheet. Part 1, Introductory note, European Chemicals Agency, 2017.

49 European Chemicals Agency, Guidance on information requirements and chemical safety assessment – Chapter 14: occupational exposure assessment, version 3.0 - August 2016, European Chemicals Agency, 2016.

50 C. Han, A. Zhao, E. Varughese and E. Sahle-Demessie, Evaluating weathering of food packaging polyethylene-nano-clay composites: Release of nanoparticles and their impacts, *NanoImpact*, 2018, **9**, 61–71.

51 W. Wohlleben, C. Kingston, J. Carter, E. Sahle-Demessie, S. Vázquez-Campos and B. Acrey, *et al.*, NanoRelease: Pilot interlaboratory comparison of a weathering protocol applied to resilient and labile polymers with and without embedded carbon nanotubes, *Carbon*, 2017, **113**, 346–360.

52 W. Wohlleben and N. Neubauer, Quantitative rates of release from weathered nanocomposites are determined across 5 orders of magnitude by the matrix, modulated by the embedded nanomaterial, *NanoImpact*, 2016, **1**, 39–45.

53 F. Doğan, K. Şirin, F. Kolcu and İ. Kaya, Conducting polymer composites based on LDPE doped with poly(aminonaphthal sulfonic acid), *J. Electrost.*, 2018, **94**, 85–93.

54 R. Vinodh, A. Abidov, M. M. Peng, C. M. Babu, M. Palanichamy and W. S. Cha, *et al.*, A new strategy to synthesize hypercross-linked conjugated polystyrene and its application towards  $\text{CO}_2$  sorption, *Fibers Polym.*, 2015, **16**(7), 1458–1467.

55 A. Di Bartolomeo, L. Iemmo, F. Urban, M. Palomba, G. Carotenuto, A. Longo, A. Sorrentino, F. Giubileo, G. Barucca and M. Rovere, *et al.*, Graphite platelet films deposited by spray technique on low density polyethylene substrates, *Mater. Today: Proc.*, 2020, **20**, 87–90.

56 M. Ibrahim, H. He and R. Chen, In situ density determination of polyethylene in multilayer polymer films using Raman microscopy, Thermo Scientific, 2017, Available from: <https://assets.thermofisher.com/TFS-Assets/MSD/Application-Notes/AN53001-in-situ-density-determination-pe-polymer-films-raman-microscopy.pdf>.

57 H. Sato, M. Shimoyama, T. Kamiya, T. Amari, S. Aic and T. Ninomiya, *et al.*, Raman spectra of high-density, low-density, and linear low-density polyethylene pellets and prediction of their physical properties by multivariate data analysis, *J. Appl. Polym. Sci.*, 2002, **86**(2), 443–448.

58 B. W. Brinkmann, L. Dupuis, S. Houdijk, P. Wattel, C. Salgado and A. Brunelli, *et al.*, Eugenol-Loaded Nanocarriers Exert Particle-Specific Adverse Effects on *Daphnia magna* Populations, *Environ. Sci. Technol.*, 2025, **59**(31), 16293–16303.

